
Article:
Du, J., Hartley, C., Brooke-Wavell, K. et al. (4 more authors) (2021) High-impact exercise stimulated localised adaptation of microarchitecture across distal tibia in postmenopausal women. Osteoporosis International, 32 (5). pp. 907-919. ISSN 0937-941X

https://doi.org/10.1007/s00198-020-05714-4

High-Impact Exercise Stimulated Localised Adaptation of Microarchitecture across Distal Tibia in Postmenopausal Women

Juan Du[1,2], Chris Hartley[3], Katherine Brooke-Wavell[3], Margaret A Paggiosi[4], Jennifer S Walsh[4], Simin Li[2] *, Vadim V Silberschmidt[2]

[1] Academy of Medical Engineering and Translational Medicine, Tianjin University, Tianjin, China

[2] Wolfson School of Mechanical, Electrical and Manufacturing Engineering, Loughborough University, Leicestershire, UK

[3] School of Sport, Exercise and Health Science, Loughborough University, Leicestershire, UK

[4] Mellanby Centre for Bone Research, University of Sheffield, Sheffield, UK

* Corresponding author. Email address: S.Li@lboro.ac.uk

Conflicts of interest/Competing interests (include appropriate disclosures)

SL received grant support from Loughborough University. KBW received grant support from NIHR Leicester Biomedical Research Centre. JSW received grant support from National Institute for Health Research. The remaining authors declare no competing financial interests.

Summary

We provided evidence that a 6-month regular hopping exercise intervention can increase trabecular number and possibly trabecular volume fraction of the distal tibia. Our novel localised analysis demonstrated region-specific changes, predominantly in the anterior region, in postmenopausal women.

Abstract

Purpose

The localisation of bone remodelling and microarchitectural adaptation to exercise loading has not been demonstrated previously in-vivo in humans. The aim of this study is to assess the feasibility of using 3D image registration and high-resolution peripheral quantitative computed tomography (HR-pQCT) to investigate the effect of high-impact exercise on human trabecular bone variables, and remodelling rate across the distal tibia.

Method

Ten postmenopausal women were recruited for 6-month unilateral hopping exercises, with HR-pQCT scans taken of both exercise leg (EL) and control leg (CL) for each participant before and after the intervention. A 3D image registration was used to ensure measurements were taken at the same region. Short-term reproducibility tests were conducted prior to the assessment using identical setup. The results were assessed comparing CL and EL, and interaction (time × leg) using a two-way repeated measures analysis of variance (RM-ANOVA).

Results

Across the whole tibia, we observed significant increases in trabecular number (Tb.N) (+4.4%), and trabecular bone formation rate (tBFR) (3.3%) and a non-significant increase in trabecular bone volume fraction (BV/TV) (+1%) in the EL. Regional resorption was higher in the CL than the EL, with this difference being statistically significant at the lateral tibia. In the EL, tBFR was significantly higher in the anterior region than the medial but a trabecular bone resorption rate (tBRR) showed no significant regional variation. Conversely in the CL, both tBFR and tBRR were significantly higher in the anterior and lateral than the medial region.

Conclusion

We demonstrated that it was possible to detect exercise related bone adaptation with 3D registration of HR-pQCT scan data. Regular hopping exercise increased Tb.N and possibly BV/TV across the whole distal tibia. A novel finding of the study was that tBFR and tBRR responses to loading were localised: changes were achieved by formation rate exceeding resorption rate in the exercise leg, both globally and at the anterior region where turnover was greatest.

Key words: Trabecular bone; Formation and resorption rates; Finite-element analysis; 3D image registration; Exercise; HR-pQCT

Introduction

Osteoporosis is a common condition where bone loss and its structural deterioration increase the risk of fracture [1]. Exercise or *in-vivo* loading could provide a strategy to counteract bone

loss and maintain its density with age, reducing the risk of fracture [2]. The distribution of bone, in addition to the density, is also important for its quality and resistance to fracture [3]. Region-specific changes in cortical bone were found at the tibial shaft as a result of physical activity [4], and local changes in cortical and trabecular bone mineral content (BMC) were demonstrated at the proximal femur, using quantitative computed tomography (QCT) in older men [5]. Trabecular microarchitecture is another determinant of bone strength [6][7]. Substantial spatial variation of trabecular bone microstructure was reported, explained by localised adaptation to regional biomechanical environment [4][8]. However, no previous research has demonstrated the location of trabecular adaptation in response to controlled exercise in humans.

Effects of exercise on trabecular microarchitecture were reported in one non-controlled-exercise study but not in a controlled intervention [9]; neither of these studies were long enough to fully capture changes in mineralisation. Exercise induced changes in remodelling rate in humans have only been examined using biomarkers [10]. The combination of a controlled-exercise study and localised microstructure analysis would provide further insight into the effect of mechanical loading on the quality and structural-functional adaptations of trabecular bone.

3D image registration was widely used in animal models to detect the loading-induced localised trabecular adaptation *in-vivo* [11] [12]. The combination of 3D registration with high-resolution peripheral quantitative computed tomography (HR-pQCT) scans to quantify *in-vivo* trabecular bone adaptation in humans is possible in theory but remains a significant challenge due to the limitation in image resolution [13]. Christen et al. used a two-step image processing after greyscale image registration to investigate the bone remodelling location; their results indicated that time-lapse *in-vivo* HR-pQCT could assess age-related bone remodelling [14]

[15]. In the current novel study, HR-pQCT was used together with a 3D rigid image registration technique to determine whether the technique could be used to detect trabecular bone adaptation to exercise. This was examined in a six-month longitudinal evaluation of the response to unilateral high-impact hopping exercise, that was already demonstrated to benefit the femoral-neck BMD [5], in the distal tibia of post-menopausal women. This model allows the advantage of comparing changes in the randomly assigned exercise leg (EL) to the control leg (CL) of the same participants. We hypothesised that trabecular bone adaptation is regional and high-impact exercise can suppress the trabecular bone resorption rate, hence, increase bone volume fraction. The primary objective of this study was to investigate the effects of a high-impact exercise intervention on global trabecular bone volume in healthy postmenopausal women. Secondary objectives were to examine localised changes in trabecular microarchitecture and localised bone remodelling rates (bone formation and resorption rates) in the EL compared to the CL.

Methods

Study design and participants

The participants were recruited from a cohort of postmenopausal women completing a randomized controlled trial of a six-month high-impact, unilateral exercise (registered at clinicaltrials.gov: NCT03225703: The Effect of High-Impact Exercise on Bone and Articular Cartilage in Postmenopausal Women). The study design, methods, and main findings of the trial have been published [16], but key methods are summarised below A subgroup of participants from this study volunteered to have HR-pQCT scans for the current study.

Inclusion criteria for the study were women aged 55-70 years who were at least 12 months post-menopause, a BMI less than 30 kg/m^2 with no diagnosis of osteoporosis or knee osteoarthritis and no other contraindications to exercise. Those that completed more than one bout of high-impact exercise per week (with likely ground reaction force greater than jogging) or taking medication known to affect bone metabolism were excluded.

The exercise intervention was a six-month unilateral hopping protocol, completed on the same randomly assigned EL to be compared with the contralateral CL[5][16]. The intervention was individually progressed for the first ten weeks, leading to the final protocol of 50 multidirectional hops daily for all participants in weeks 11-26. The hops were split into 3-5 sets with 15 s of rest between each set. Adherence was assessed by diary. To detect sufficient changes in mineralization, a six-month trial period was selected as the minimum duration for bone adaptation is approximately four months [17][18]. HR-pQCT scans were taken at baseline and after six months of the exercise intervention by an experienced operator who was blinded to the EL allocation. All data were analysed by a single researcher, also blinded to the EL allocation.

The study was approved by the National Research Ethics Service (16/EM/0460) and Loughborough University Ethics Approvals (Human Participants) Sub-Committee (R16-P149). Written informed consent was obtained from all the participants at the first meeting, prior to enrolment in the study.

HR-pQCT imaging

HR-pQCT (XtremeCT, Scanco Medical) scans were performed at pre- and post-intervention for each participant, using the manufacturer's standard *in-vivo* protocol [19] (60 kVp, 1000 mA,

100-ms integration time), by the same operator at the NIHR Clinical Research Facility, Sheffield Teaching Hospitals NHS Foundation Trust, Sheffield. Prior to image acquisition, each participant's tibia was immobilized in a carbon-fibre mould and fixed within the scanner to ensure a correct position upon entry. The region of interest was defined as 110 parallel CT slices, started 22.5 mm proximal to the distal tibia endplate and ended at a further 9.02 mm proximal to the site. A field of view of 12.6 cm was reconstructed across a 1536 × 1536 matrix, yielding an isotropic voxel size of 82 μm [20]. For quality control, linear attenuation of the phantom was converted to hydroxyapatite (HA) densities and calibrated on a daily basis following manufacturer's standard method. A post-scan quality check was assessed, using a manufacturer-recommended method to categorise the images from perfect (G1) to unacceptable (G4). Images defined as G4 were rejected for any further analysis, to ensure only good-quality images were used.

Image registration and regional analysis

A 3D rigid registration protocol similar to that described previously [14] was used to obtain a common volume of interest (VOI) between pre- and post-intervention scans. Two steps were involved in this registration process (Fig. 1A): first, the centre of mass of the entire tibia from both the follow-up and baseline scans were pre-aligned; second, the pre-aligned follow-up images were registered to the baseline images using a normalized mutual information metric and resampled using a Lanczos interpolator. Previous studies showed the effect of the Lanczos interpolator was minimal to HR-pQCT scans [21]. The registration and resample process ensured the largest common volume and, importantly, the same coordinate system.

In order to observe the region-specific information, four anatomic regions were defined according to the process described previously [22]. In brief, a horizontal line was drawn

through the centre of a circle, used to define the tibia area; two lines at ± 45° to the horizontal line were used to separate four anatomical regions (anterior, lateral, posterior, medial). To minimize selection bias, a custom developed cropping procedure for defining cubic representative volume elements (RVEs) with a side-length of 4 mm was performed on the common volume between the baseline and follow-up scans (Fig. 1B). The selected RVEs were evenly distributed, either along the centre line of each region or spread at equal distances away from the inner surface of the cortical bone for each participant. All cubes were carefully visually checked to ensure that they had no cortical bone.

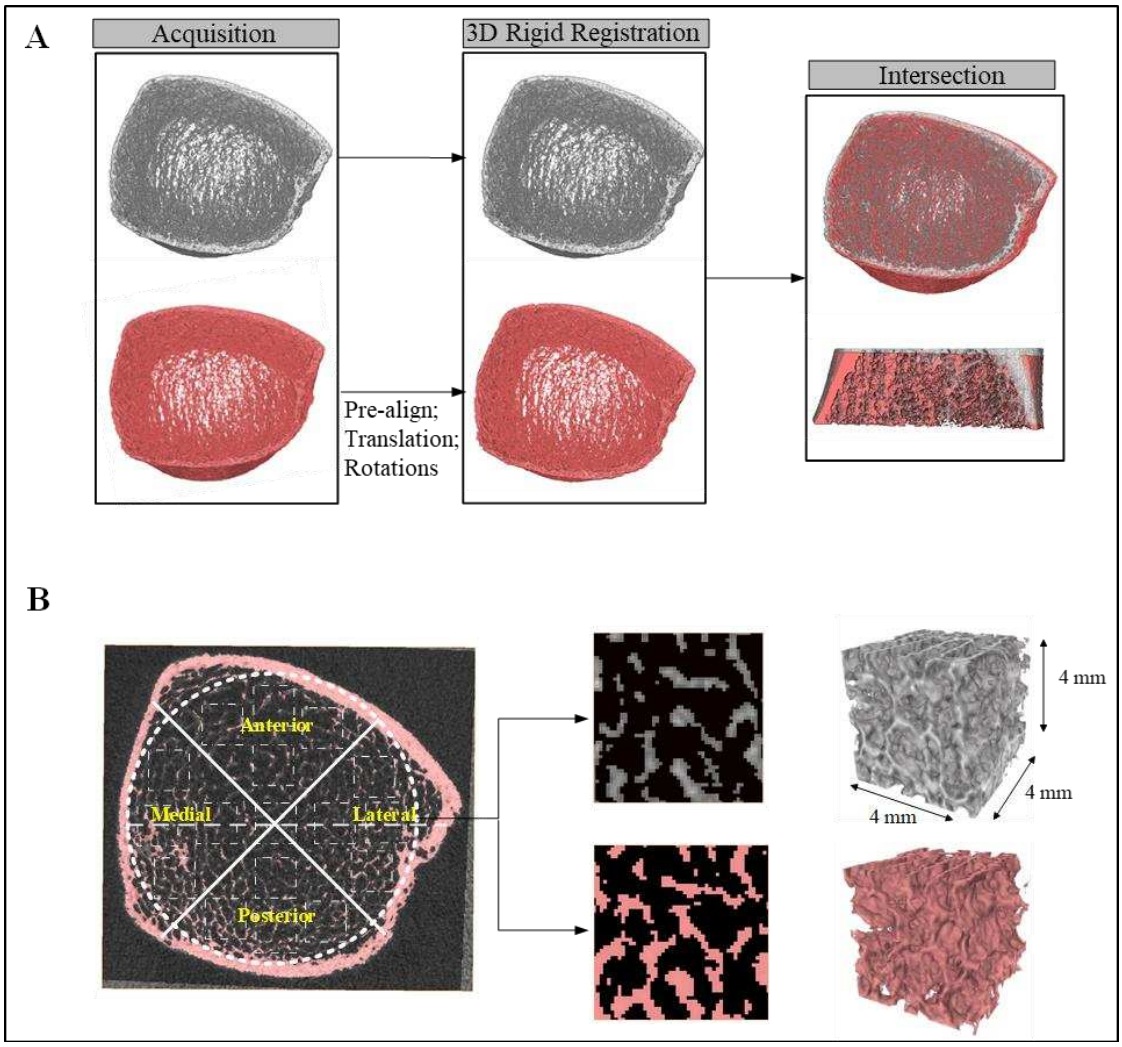

Figure 1: Methodology for registration and identifying anatomical regions for baseline and follow-up images. (A) Rigid registration of follow-up scans (red) to baseline images (grey). (B) Definition of anatomical regions and locations of RVEs for distal tibia in common regions of baseline and follow-up scans.

Trabecular remodelling analysis

HR-pQCT images were Laplace-Hamming filtered, as recommended by the manufacturer, producing an adequate balance between the sensitivity and noise present in the measurements [21]. Remodelling parameters of trabecular bone were computed from the superimposed binary images obtained from the baseline and follow-up scans. After the 3D registration process, the common VOI could be identified at both time points, allowing the quantification of morphometric changes in the trabecular bone compartment (Fig. 2). From the overlaid images, site-specific spatial-temporal changes of individual RVEs were categorized simultaneously through triangulation (Boolean operation) between the baseline and follow-up images. Bone resorption and formation were defined as voxels present only in the baseline images (green) or only in the follow-up images (magenta), respectively; while the voxels present in both images were identified as quiescent bone (grey). These colour-coded datasets were used directly to quantify dynamics of trabecular remodelling using a MATLAB routine. The trabecular bone resorption rate (tBRR) was calculated as the ratio of volume of green voxels to the total volume of bone voxels per month, whereas the bone formation rate (tBFR) was defined similarly employing the volume of magenta voxels; the unit for both parameters is %/month.

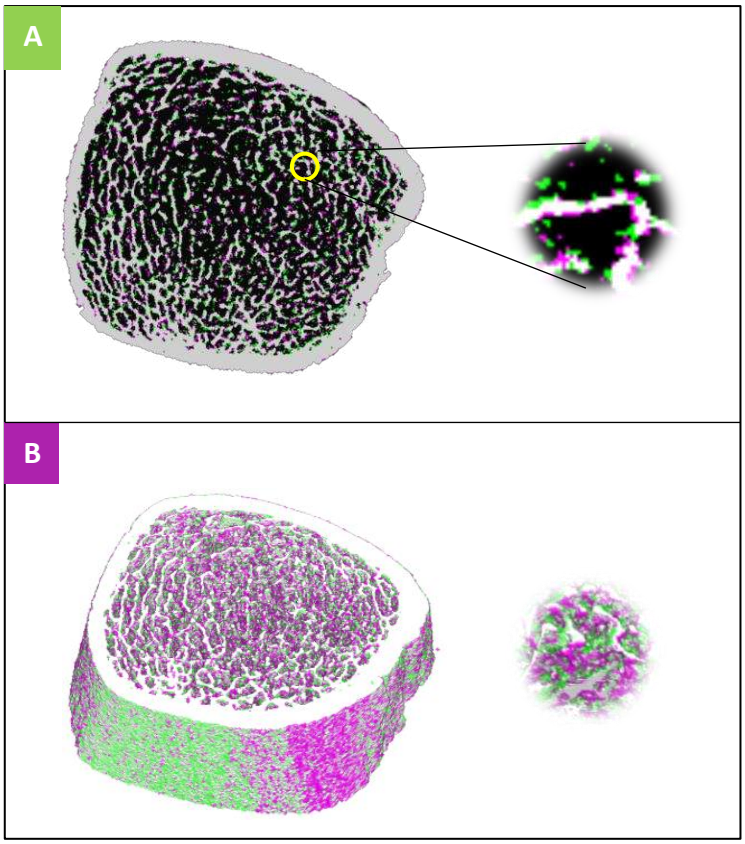

Figure 2: Typical registered 3D whole bone images: (A) cross-section of overlaid images of baseline and follow-up scans, with black and white representing marrow and bone regions, respectively; (B) 3D view of sites of bone resorption (in green) and formation (in magenta).

Analysis of microstructural variables

Trabecular compartments were segmented and reconstructed using Materialise Mimics Innovation Suite 19.0 (Materialise, Leuven, Belgium) based on a fixed threshold of 300 mg HA/cm^3 [23]. The microstructure of extracted trabecular compartments was analysed using BoneJ, an open-source bone–image-analysis plugin in ImageJ [24]. In addition to the standard HR-pQCT patient evaluation protocol to assess the whole-bone variables, a direct image-analysis protocol implemented in BoneJ (described previously [22][24]) was used to analyse localised microstructural variables of trabecular bone. The trabecular bone volume fraction (BV/TV) was calculated from the number of foreground (bone) voxels divided by the total number of voxels in the image. The trabecular number (Tb.N) was the inverse of the diameter of the sphere that fits the ridges between trabeculae [25] . Trabecular thickness (Tb.Th) was

the largest sphere that fits within a trabecula [25]. The trabecular bone surface area (Tb.BS) was the sum of the areas of the triangles making up a surface mesh [27]. The ratio of plate-like structures to the total number of trabecular structures ($_{P}$Tb.N/$_{T}$Tb.N), was defined when the ellipsoid factor (EF) calculated in BoneJ for the given space was in the range between −1 and 0, i.e. producing a flattened (oblate) ellipsoid as the number of fitting ellipsoids for the plate-like trabeculae divided by the total number of fitting ellipsoids [22][28].

Finite-element analysis

Two-phase finite-element models of trabecular bone and surrounding bone marrow were developed based on the RVEs taken from the anatomic regions of registered HR-pQCT images. A voxel-based tetrahedral mesh [29] was used to generate finite-element meshes of both trabecular bone and bone marrow using 3-Matic 11.0 (Materialize, Leuven, Belgium). An isotropic, linear-elastic material with the Young's modulus of 15 GPa and 3 MPa and the Poisson's ratio of 0.3 and 0.17 were assigned to the bone and marrow materials, respectively [30]. A uniaxial compressive strain of 1% was applied in the axial direction at the proximal surface of the trabecular bone to compute the stiffness (kN/mm) of each RVE, which was calculated by dividing the reaction force of the proximal surface by the corresponding displacement. The numerical computations were performed on a workstation (HP Z440) using Abaqus 6.14 software (Dassault Systems Simulia Crop, Providence, RI, USA).

Reproducibility test

A previous reproducibility data set from Paggiosi et al. [20], in which two repeated scans of ten participants from 70 years of age cohort were taken on the same day, was used to assess the short-term reproducibility of variables examined in the current study. The data set was

obtained using the same image acquisition setup and protocol from the same laboratory as this study. The short-term reproducibility of all the microstructural variables was calculated as the root mean square coefficient of variance (RMSCV%). The least significant detectable change (LSC) was calculated as LSC = 2.77×RMSCV. The reproducibility was between 1.6%-3.3% (RMSCV%) and 0.044%-0.093% for all the local microstructural parameters and 3.0% for stiffness, while the precision error of the global parameters was between 0.2–5.3 % [20]. The RMSCV% and LSC for bone remodelling rate were 2.1% and 1%/month, respectively. Christen et al. [15] reported that the LSC for local bone remodelling of 2% was small enough to capture even minor changes in the bone microstructure.

Statistical analysis

Results are presented here as mean ± SD (absolute value) and 95% CI (percentage change) at both global and regional (anterior, lateral, posterior, medial) levels. Data distributions were assessed by examination of normality plots, and Mauchly's test was used to assess sphericity. The effect of high-impact, unilateral hopping exercise on microstructural variables and stiffness of regional trabecular bone over time, between control and exercise legs, as well as their interaction (time × leg) were assessed at each anatomical region using two-way repeated measures analysis of variance (RM-ANOVA) (Table 1). P values were adjusted using Bonferroni corrections for all the multiple comparisons, keeping the critical level of significance consistently at 0.05.

Changes in all the studied parameters were calculated between the baseline and follow-up scans and expressed as percentage difference to normalise variation in magnitude for illustration and comparison purposes. Comparisons 1) between legs and 2) among anatomical regions within each leg were performed using one-way RM-ANOVA to evaluate statistical significance.

Significance level was set at $p < 0.05$, and all the statistical analyses were conducted using SPSS Statistics 20.0 software (IBM Corp., NY, USA).

Results

Effect of exercise on microstructural variables and stiffness

Ten participants were recruited to the study aged (mean ± SD) 63 ± 4 years, with height of 1.62 ± 0.05 m, body mass 66.4 ± 10.0 kg and BMI 25.4 ± 3.7 kgm^{-2}. One participant withdrew prior to follow up, but all others had data pre- and post- intervention scans. Data of thirty-six RVEs (n = 36) in each leg were analysed for the remaining 9 participants (age 62.6±4.1 years; BMI 25.4±3.7; 10.9±4.1 years since menopause). The mean adherence for the group was 80.4 ± 24.0% during the final 14 weeks of the exercise, where the prescribed exercise consisted of 50 multidirectional hops each day. There were no significant changes in post-intervention compared with pre-intervention for body mass or height.

Global changes

Following the prescribed 6-months exercise, microstructural variables of trabecular bone from pre- and post-interventions were analysed after implementation of the 3D registration process, to ensure only the common ROIs were analysed [13]. Across the whole tibia, there was a significant increase of trabecular number (Tb.N) in the EL (from 1.70 ± 0.13 to 1.78 ± 0.20; time × leg interaction $p = 0.043$; effect size = 0.52) compared with a -0.7% reduction from 1.77 ± 0.18 to 1.75 ± 0.18 in CL (Fig.3 and Table 1). Changes in trabecular bone volume fraction (BV/TV) were higher in the EL (+1%) than the CL (+0.1%) with $p = 0.015$ (Fig. 3).

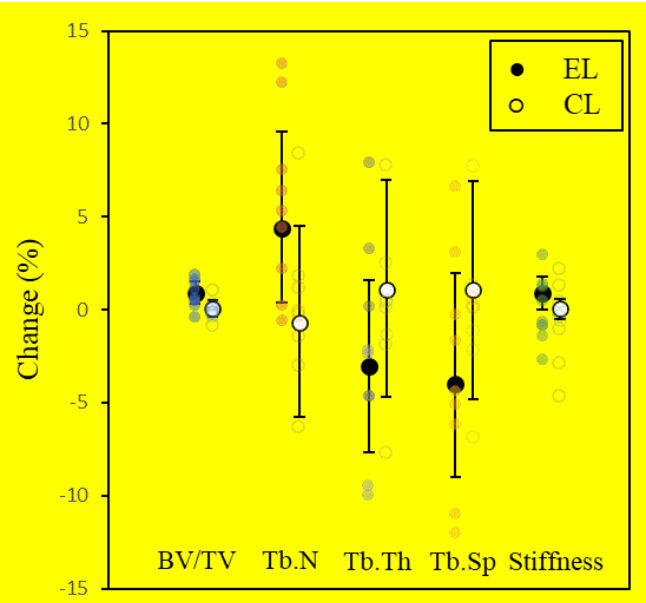

Figure 3: Global percentage changes between post- and pre-exercise of trabecular bone parameters in EL (black circle) and CL (white circle) with overlaid individual difference for each participant. Results are presented as mean ± 95% confidence interval (CI). RM-ANOVA was used to compare the percentage change between the baseline and the follow-up value.

Regional changes

For all analysed RVEs, consistent increases in BV/TV (up to +8%) were observed in the EL group, while most RVEs in the CL group showed negative changes (Appendix II). Regionally, there was a significant increase in BV/TV in the EL (+6.1%; time × leg interaction $p = 0.012$) relative to the CL (-1.9%) in the anterior region as a result of the intervention (Table 1). Similarly, the change in the trabecular number (Tb.N) in the anterior region was of the same magnitude (+6.1 vs. -2.2%) and differed considerably between the legs. This, in turn, was linked to the significant decrease in trabecular separation (Tb.Sp; time × leg interaction $p = 0.012$) observed in the anterior region between the EL and CL groups. No trend was observed for the plate-like structure fraction ($_{P}$Tb.N/$_{T}$Tb.N), with arbitrarily distributed growth and reduction in both the EL and the CL.

Table 1: Microstructural variables and stiffness of trabecular bone at pre- intervention, change after intervention and difference between anterior, lateral, posterior and medial regions

		Trabecular volume fraction (BV/TV)	Trabecular thickness (Tb.Th) [mm]	Trabecular separation (Tb.Sp) [mm]	Trabecular number (Tb.N) [1/mm]	Trabecular surface area (Tb.BS) [mm^2]	Plate-like structure fraction ($_PTb.N/_TTb.N$)	Trabecular stiffness [KN/mm]
Global								
EL	Pre	0.126 ± 0.015	0.074 ± 0.011	0.519 ± 0.047	**1.698 ± 0.131**[b]	-	-	176.35 ± 19.19
	Post	0.127 ± 0.020	0.071 ± 0.014	0.498 ± 0.068	**1.779 ± 0.201**[b]			173.85 ± 18.97
	Δ %	0.8 (0.1, 1.5)	-3.0 (-7.7, 1.6)	-4.0 (-8.8, 0.8)	4.4 (-0.7, 9.6)	-	-	-1.4 (-3.7, 0.9)
CL	Pre	0.126 ± 0.020	0.071 ± 0.012	0.500 ± 0.055	**1.768 ± 0.184**[b]	-	-	176.35 ± 20.30
	Post	0.126 ± 0.017	0.072 ± 0.005	0.504 ± 0.060	**1.753 ± 0.180**[b]			176.12 ± 19.78
	Δ %	0.1 (-0.4, 0.5)	1.1 (-4.7, 7.0)	1.1 (-4.8, 6.9)	-0.7 (-5.8, 4.5)	-	-	-0.1 (-1.3, 1.1)
Anterior								
EL	Pre	**0.208 ± 0.092**[bc]	**0.300 ± 0.048**[a]	**0.772 ± 0.141**[bc]	**1.335 ± 0.231**[b]	123.028 ± 48.731	0.483 ± 0.165	4.060 ± 4.422
	Post	**0.222 ± 0.090**[bc]	**0.282 ± 0.052**[a]	**0.734 ± 0.150**[bc]	**1.418 ± 0.282**[b]	128.256 ± 50.970	0.489 ± 0.160	4.375 ± 4.907
	Δ %	6.1 (-5.0, 17.2)	-5.9 (-11.0, -0.8)	-5.0(-11.3, 1.3)	6.1 (-1.7, 13.9)	4.3 (-0.6, 9.2)	8.7 (-4.3, 21.7)	5.9 (-17.2, 29)
CL	Pre	**0.217 ± 0.090**[bc]	**0.292 ± 0.04**[a]	**0.727 ± 0.138**[bc]	**1.423 ± 0.257**[b]	127.946 ± 48.293	0.500 ± 0.179	4.537 ± 4.610
	Post	**0.214 ± 0.092**[bc]	**0.279 ± 0.05**[a]	**0.745 ± 0.141**[bc]	**1.391 ± 0.259**[b]	126.997 ± 48.138	0.485 ± 0.175	4.334 ± 4.987
	Δ %	-1.9 (-3.8, 0.0)	-4.3 (-9.6, 1.0)	2.6 (-2.6, 7.9)	-2.2 (-6.8, 2.4)	-1.1 (-5.1, 3.0)	-0.7 (-9.7, 8.4)	-2.4(-11.4, 6.6)
Lateral								
EL	Pre	0.271 ± 0.080	0.301 ± 0.044	0.604 ± 0.118	1.714 ± 0.297	162.921 ± 43.274	0.552 ± 0.174	7.167 ± 4.372
	Post	0.287 ± 0.096	0.290 ± 0.287	0.580 ± 0.120	1.797 ± 0.362	165.198 ± 45.589	0.552 ± 0.147	8.849 ± 6.677
	Δ %	5.2 (-4.6, 15.0)	-3.8 (-9.2, 1.5)	-3.9 (-9.6, 1.8)	4.8 (-2.2, 11.7)	1.4 (-1.8, 4.6)	0.0 (-1.6, 1.5)	17.2 (0.4, 10.3)
CL	Pre	0.269 ± 0.078	0.293 ± 0.030	0.605 ± 0.118	1.715 ± 0.319	164.567 ± 43.166	0.539 ± 0.169	7.053 ± 4.310
	Post	0.267 ± 0.084	0.282 ± 0.032	0.609 ± 0.120	1.705 ± 0.316	163.786 ± 42.949	0.539 ± 0.139	7.018 ± 4.688
	Δ %	-1.0 (-2.7, 0.6)	-3.6 (-8.1, 0.9)	0.8 (-2.8, 4.4)	-0.6 (-3.9, 2.8)	-0.5 (-1.6, 0.7)	0.2 (-3.8, 10.8)	-0.3 (-10.0,9.4)
Posterior								
EL	Pre	0.307 ± 0.101	0.319 ± 0.040	0.577 ± 0.133	1.816 ± 0.371	168.382 ± 43.971	0.583 ± 0.15	10.050 ± 5.951
	Post	0.313 ± 0.114	0.314 ± 0.072	0.566 ± 0.138	1.862 ± 0.400	170.646 ± 44.995	0.547 ± 0.16	10.700 ± 6.910
	Δ %	1.9 (-1.1, 4.9)	-1.7(-10.1, 6.8)	-2.1 (-5.9, 1.6)	2.4 (-1.4, 6.3)	1.3 (-0.2, 2.7)	-2.2(-11.8, 7.5)	6.1(-2.9, 15.2)
CL	Pre	0.321 ± 0.114	0.321 ± 0.050	0.553 ± 0.12	1.884 ± 0.364	178.029 ± 47.600	0.600 ± 0.152	10.629 ± 5.721
	Post	0.320 ± 0.112	0.309 ± 0.046	0.551 ± 0.12	1.892 ± 0.371	177.727 ± 47.791	0.580 ± 0.153	9.918 ± 6.240
	Δ %	-0.4 (-2.1, 1.3)	-3.8 (-8.1, 0.6)	-0.2 (-4.5, 4.1)	0.5 (-3.6, 4.7)	-0.6 (-2.6, 1.4)	-0.2 (-7.8, 7.4)	-5.2(-24.1 ,6.6)
Medial								
EL	Pre	0.316 ± 0.100	**0.341 ± 0.051**[a]	0.625 ± 0.124	1.661 ± 0.331	172.106 ± 40.875	0.609 ± 0.181	10.262 ± 6.387
	Post	0.318 ± 0.105	**0.326 ± 0.060**[a]	0.608 ± 0.120	1.713 ± 0.345	172.225 ± 44.244	0.608 ± 0.170	10.387 ± 6.470

	Δ %	0.4 (-2.6, 3.4)	-4.6 (-8.9, -0.3)	-2.8 (-6.1, 0.5)	3.1 (-0.3, 6.6)	0.1 (-3.6, 3.8)	-1.2 (-5.6, 3.1)	0.4 (-8.6, 9.4)
CL	Pre	0.327 ± 0.110	**0.345 ± 0.045**[a]	0.613 ± 0.134	1.703 ± 0.330	180.813 ± 45.545	0.624 ± 0.177	10.441 ± 6.286
	Post	0.326 ± 0.102	**0.331 ± 0.050**[a]	0.610 ± 0.139	1.717 ± 0.355	177.134 ± 43.180	0.605 ± 0.181	9.265 ± 6.240
	Δ %	-0.2 (-3.0, 2.5)	-4.0 (-8.2, 0.2)	-0.3 (-6.0, 5.3)	1.3 (-1.4, 3.6)	-1.2 (5.6, 3.1)	-3.9(-8.4, 6.1)	-5.5(-14.0, 3.0)

Absolute values are expressed as mean ± standard deviation; Δ indicates change in percentage to 6-month and expressed as 95% CI; [a] significant difference in time, [b] significant difference in leg, [c] significant difference in time × leg

Effect of exercise on bone remodelling rates

Across the distal tibia, significantly higher tBFR (3.3% ± 0.5; p = 0.009) than tBRR (3.1% ± 0.4) was observed in EL (Table 2). Within the control leg, the level of tBFR (4.0%-7.1%) tended to be equal, or slightly lower than the tBRR (4.0%-7.3%) of the same location (Appendix I). Among the anatomical regions in CL (Fig. 4), levels of tBRR were significantly higher in the anterior (6.5% ± 2.0, p = 0.005) and lateral (5.9% ± 1.5, p = 0.001) regions than that in the medial (4.7% ± 1.4) region. Whereas, in the exercise leg, tBFR (4.2%-7.2%) tended to be higher than tBRR (4.0%-6.3%) of the same location (Appendix I), with the anterior region having a significantly higher level of tBFR (6.4% ± 1.8, p = 0.028) than tBRR (5.7% ± 1.8) (Table 2). Regional comparisons showed no significant regional differences of tBRR within the EL (Fig. 4) but tBFR was significantly higher in the anterior region (6.4% ± 1.8, p= 0.013) than in the medial one (4.8% ± 1.4) in the EL group. Between the EL and CL groups, tBRR tended to be lower (or maintained) in the EL with a significantly lower tBRR in the lateral region (5.17% ± 1.3, p = 0.033) compared with the CL (5.89% ± 1.48) (Table 2), whilst tBFR tended to be higher (or maintained) in the EL relative to the CL.

Table 2: Absolute values of trabecular bone formation rate (tBFR) and bone resorption rate (tBRR) after 6-month exercise.

	tBFR (%/month)	tBRR (%/month)
Global		
EL	3.26 ± 0.52 [b]	3.07 ± 0.43 [b]
CL	3.16 ± 0.64	3.23 ± 0.57
Regional		

Anterior		
EL	6.42 ± 1.78[b]	5.68 ± 1.81[b]
CL	6.25 ± 1.86	6.51 ± 2.02
Lateral		
EL	5.80 ± 1.11	5.17 ± 1.32[a]
CL	5.71 ± 1.36	5.89 ± 1.48[a]
Posterior		
EL	5.32 ± 1.31	5.06 ± 1.14
CL	5.24 ± 1.59	5.42 ± 1.69
Medial		
EL	4.83 ± 1.41	4.61 ± 1.22
CL	4.55 ± 1.42	4.71 ± 1.35

Data are expressed as mean ± standard deviation; one-way RMANOVA was used to compare the difference: (1) between tBFR and tBRR within each leg; (2) between legs.

[a] significant difference between EL and CL

[b] significant difference between tBFR and tBRR

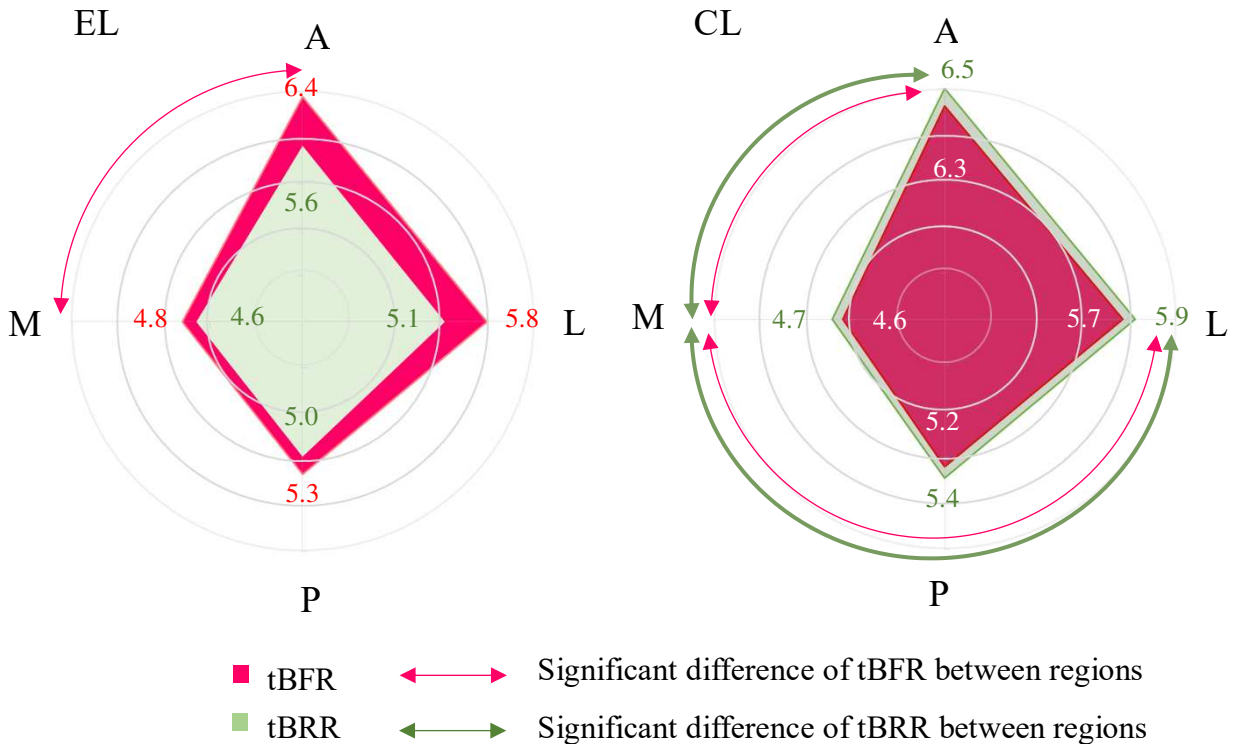

Figure 4: Variation of tBFR and tBRR across anatomic regions: A (anterior), P (posterior), L (lateral) and M (medial) in EL and CL. Regional comparisons within each leg were conducted using one-way RMANOVA (Significant differences between regions were

indicated and linked using double-sided arrows; the values representing the scale of the gridlines are from 3.0% to 6.5%).

Discussion

This study demonstrated that high-impact exercise can induce both global and regional changes in remodelling rate, microstructure and mechanical competence of trabecular bone in human distal tibia. Following 6-months of exercise, there were significant improvements in Tb.N and possibly BV/TV across the distal tibia in the EL relative to the CL, with significantly higher net bone turnover (tBFR significantly higher than tBRR) observed in EL. Using 3D rigid registration of HR-pQCT scans, it was revealed for the first-time that these global changes were associated with a lower bone resorption rate of the EL relative to the CL in the antero-lateral region, with parallel increases in anterior BV/TV, Tb.N, and reduction in Tb.Sp. Also, it was demonstrated that the exercise-induced trabecular adaptations and changes in microstructure varied across the distal tibia, with substantial improvements in the anterior region.

One of the novel components of the study was the use of 3D rigid registration and regional analysis to provide local measurements of the bone remodelling rate across the distal tibia. Significant regional differences were evident: the control leg demonstrated both higher formation and resorption in the anterior (6.25% and 6.51%) and lateral regions (5.71% and 5.89%), respectively, than in the medial tibia (4.55% and 4.71%). The exercise appeared to suppress bone resorption in EL, particularly in the antero-lateral tibia, so that resorption did not differ regionally, although the bone formation remained significantly greater (+25%) in the anterior than medial tibia. Our findings suggest that the postmenopausal bone remodelling rate across the distal tibia has a spatially non-uniform distribution, with the anterior and lateral regions being particularly active remodelling parts, both in terms of bone resorption and

formation. The hopping intervention suppressed the remodelling process by shifting away from a pro-resorption regime towards a formation-dominant process. It is possible that the regional suppression in the antero-lateral region was the result of the elevated and non-uniform strain and strain rate, experienced at this site during the multidirectional high-impact exercise [31][32]. Sode et al. also reported a significantly larger loss of trabecular structure in the antero-lateral region of the distal tibia in women aged between 65-79 [8], and the loss of mechanical integrity may result in higher strains induced during exercise at this region and hence more adaptation to mechanical loading. Although no significant effects on bone formation in postmenopausal women were observed, some animal studies reported that mechanical loading affected both the formation and resorption rates [33][34]. Interestingly, our results also suggest that this jumping intervention could help to balance the resorption rate between the regions, especially, an improvement in bone quality was found in the anterior region for the first-time, which was reported as the "weakest" region of the distal tibia before [8][35]. Furthermore, the magnitude of the reduction in the resorption rate reported in this study was consistent with that observed using biomarkers during a three-year follow-up study of anti-resorptive (bisphosphonate) treatment [36][37], however, without the potential side effects caused by drugs.

The trabecular bone volume fraction and number were increased and maintained in the exercise leg but tended to decline in the control leg. Among the EL regions, there were significant increases up to +6.1% and +6.1% in BV/TV and Tb.N, respectively, accompanied by -5.9% and -5.0% reduction in Tb.Th and Tb.Sp. In contrast, no significant change was observed in the CL, consistent with the observation of unaltered Tb.Th in ageing bone [38][39][40]. Explanations for this might be that the exercise resulted in the formation of trabeculae with lower thickness initially, or trabecular separation/branching from the existing trabeculae. This

suggestion is supported by our observation that Tb.N increased more in the EL than CL. Gabet et al. further suggested that the unaltered Tb.Th in aging skeleton may originate from two sources: (i) a biased measurement incorporating the cortical remnants, generated from the cortical bone resorption process, i.e., trabecularization of the cortex; (ii) the early clearance of thin trabecular struts [41]. Our results support the hypothesis that mechanical loading might efficiently reduce the trabecularization of the cortex as a result, suppressing the cortical resorption process. This suggestion is further supported by local increases in the cortical mass surface density of proximal femur in our previous study [5]. A proof of this requires further analyses of cortical bone as well as trabecular changes.

The effects of physical exercise on the distal tibia measured with HR-pQCT was examined previously. In particular, the observed localised increases in BV/TV and Tb.N in our study are consistent with changes in response to jumping activity, previously reported for boys [4]. However, a recent study with postmenopausal women using a shorter, 3-month intervention observed improvements only in mechanical properties, while no significant changes in trabecular microarchitecture were found [42]. This was, probably, because this duration was insufficient for the necessary changes in mineralisation to be detected with HR-pQCT. On the other hand, another study [9], with a cohort of women aged 21.5 ± 3.3 yrs subjected to 8-week US army basic combat training, led to significant improvements in trabecular bone microarchitecture and bone strength measured following the standard HR-pQCT protocol. It is possible that the cohort age, exercise intensity, duration and study design, as well as the adopted measurement technique, differed for these studies. Yet, the benefits of physical exercise on bone health in general are profoundly evident across all studies. By implementing a 3D rigid registration analysis, it was possible to observe a clear shift in the remodelling process of the human distal tibia in response to physical exercise for the first-time. Further studies may be

required to investigate the sensitivity of bone remodelling rate to different factors in order to understand and deliver targeted benefits to different cohorts.

One benefit of using local trabecular measurement is its capability to detect minor and region-specific changes that otherwise cannot be detected based on mean values provided by the global HR-pQCT measurement across the whole tibia area [8][35][4]. One possible implication of this study is that regional variations in the changes of bone resorption and formation may help to improve our understanding of the structural-function evolution in the development of early osteoporosis, especially in regions prone to deterioration, such as the anterior region [8][43].

A radical change of trabecular structure from plate-like to rod-like was reported in ageing and osteoporotic cohort studies [44][45]. However, in our study, non-consistent changes between the plate-like and rod-like structures in the non-osteoporotic cohort were found. We conjecture that the bone remodelling process in healthy, and ageing/osteoporotic cohorts maybe subject to different regulation pathways. The changes in plate-like and rod-like structures only partially reflect the morphological variations of trabecular microarchitecture. Further assessment of their orientation distribution such as those reported in [46][47] could be performed for an additional insight.

This study has strengths in the novel variables assessed and the unilateral design that provided a well-matched control limb, but some limitations warrant acknowledgement. First, the number of participants who completed the 6-month intervention was only nine; however, a total of 36 ROI was extracted on each region to analyse the regional difference, the well-matched control limb increases statistical power and findings were adjusted for multiple comparisons. The study provides preliminary data needed to support further larger cohort studies. Secondly, it is possible that the hopping intervention influenced the control limb also, due to changes in

activity during the intervention or any systemic musculoskeletal effects. But in previous research changes in the control leg did not differ from changes in a randomly assigned control group [48]. Another factor was that the intervention was only for six months, possibly limiting the magnitude of trabecular bone variables reported. However, results from previous research demonstrated that this was adequate to detect changes in femoral neck BMD [5], and the current study demonstrates that six-month intervention was long enough to register trabecular adaptations across distal tibia. Furthermore, the stiffness predicted with FE simulations did not include the effect of spatial variations of bone mineral density at individual voxel level, hence, may offset the accuracy of the predicted stiffness changes. Nonetheless, the reported relative changes outweigh the importance of their absolute values; it is recommended that FE analysis performed in this and in other HR-pQCT-based studies can be further improved by implementing spatially non-uniform material properties based on measurements of bone mineral density for individual voxels. Last but not least, the report of absolute values of microstructural and bone remodelling parameters may also be limited by the spatial resolution (82 μm voxel size) of HR-pQCT images. In addition, the current registration method requires rotation of the images into the same coordinate system, which may introduce interpolation bias [13][33]. However, our short-term reproducibility study showed that the RMSCV% value was below 3.4% and comparable with reproducibility of other HR-pQCT analyses [33][49]. New methods of image registration to reduce interpolation biases [50] [15] might improve the accuracy of absolute values for further studies.

In summary, we provided evidence that a 6-month high-impact exercise intervention can increase trabecular number and may improve trabecular volume fraction of the distal tibia. Our novel localised analysis demonstrated region-specific changes predominantly in the anterior region in postmenopausal women. This is the first study to examine effects of exercise on the

remodelling rates across the distal tibia, demonstrating significant higher formation than resorption rate as a result of exercise, with suppression of the resorption rate particularly in the antero-lateral region. These local changes in trabecular microstructure and stiffness, in conjunction with the observed changes in adaptation as a result of high-impact exercise may offer further insight into the structural-function relationship and load adaptation process of human skeleton tissue. In addition, it is also plausible to conclude from this study along with previous evidence that impact exercise may offer an effective intervention strategy to produce beneficial microarchitectural as well as global adaptation that may reduce risk of osteoporosis and distal tibia stress fracture.

Declarations

Acknowledgement

The authors would like to thank all participants involved in this study as well as Ganggang Xiang, Yaqi Qian and Chenguang Zhao from Loughborough University, for their contribution in segmenting the images. We would also like to acknowledge the Mellanby Centre for Bone Research at The University of Sheffield and the NIHR Clinical Research Facility, Sheffield Teaching Hospitals for providing access to the HR-pQCT scanner.

Funding

This study was jointly supported by the Loughborough University Health & Wellbeing Research Challenge Seed Corn fund and the NIHR Leicester Biomedical Research Centre.

Conflicts of interest/Competing interests (include appropriate disclosures)

SL received grant support from Loughborough University. KBW received grant support from NIHR Leicester Biomedical Research Centre. JSW received grant support from National Institute for Health Research. The remaining authors declare no competing financial interests.

Ethics approval (include appropriate approvals or waivers)

The present study was registered at clinicaltrials.gov: NCT03225703: The Effect of High-Impact Exercise on Bone and Articular Cartilage in Postmenopausal Women.

Consent to participate (include appropriate statements)

All participants provided written informed consent.

Consent for publication (include appropriate statements)

All participants provided written informed consent for publication.

Availability of data and material (data transparency)

Data and material are not available

Code availability (software application or custom code)

Mimics, Abaqus and Matlab were used with official license. Custom code is not available.

Authors' roles

Study design: JD, SL, CH and KBW. Study conduct: JD, CH and MAP. Data collection: JD, CH, MAP and JW. Data analysis: JD and CH. Data interpretation: JD, CH, SL and KBW. Drafting manuscript: JD, CH and SL. Revising manuscript content: JD, SL, KBW and VVS. Approving final version of manuscript: all authors. JD takes responsibility for the integrity of the data analysis.

References

1. Consensus development conference: Diagnosis, prophylaxis, and treatment of osteoporosis. *Am J Med*. Elsevier; 1993 Jun 1;94(6), 646–50.

2. Lacombe J., Cairns B.J., Green J., Reeves G.K., Beral V., Armstrong M.E.G. The Effects of Age, Adiposity, and Physical Activity on the Risk of Seven Site-Specific Fractures in Postmenopausal Women. *J Bone Miner Res*. 2016;31(8), 1559–68.

3. Crabtree N., Loveridge N., Parker M., Rushton N., Power J., Bell K.L., et al. Intracapsular hip fracture and the region-specific loss of cortical bone: Analysis by peripheral quantitative computed tomography. *J Bone Miner Res*. 2001;16(7), 1318–28.

4. Macdonald H.M., Cooper D.M.L., McKay H.A. Anterior-posterior bending strength at the tibial shaft increases with physical activity in boys: Evidence for non-uniform geometric adaptation. *Osteoporos Int*. 2009;20(1), 61–70.

5. Allison S.J., Poole K.E.S., Treece G.M., Gee A.H., Tonkin C., Rennie W.J., et al. The influence of high-impact exercise on cortical and trabecular bone mineral content and 3D distribution across the proximal femur in older men: A randomized controlled unilateral intervention. *J Bone Miner Res*. 2015;30(9), 1709–16.

6. Nishiyama K.K., Macdonald H.M., Hanley D.A., Boyd S.K. Women with previous fragility fractures can be classified based on bone microarchitecture and finite element analysis measured with HR-pQCT. *Osteoporos Int*. 2013;24(5), 1733–40.

7. Stuck A.K., Schenk D., Zysset P., Bütikofer L., Mathis A., Lippuner K. Reference values and clinical predictors of bone strength for HR-pQCT-based distal radius and tibia strength assessments in women and men. Osteoporosis International; 2020;

8. Sode M., Burghardt A.J., Kazakia G.J., Link T.M., Majumdar S. Regional variations of gender-specific and age-related differences in trabecular bone structure of the distal radius and tibia. *Bone*. Elsevier Inc.; 2010;46(6), 1652–60.

9. Hughes J.M., Gaffney-Stomberg E., Guerriere K.I., Taylor K.M., Popp K.L., Xu C., et al. Changes in tibial bone microarchitecture in female recruits in response to 8 weeks of U.S. Army Basic Combat Training. *Bone*. 2018;113(December 2017), 9–16.

10. Kawalilak C.E., Johnston J.D., Olszynski W.P., Kontulainen S.A. Characterizing microarchitectural changes at the distal radius and tibia in postmenopausal women using HR-pQCT. *Osteoporos Int*. 2014;25(8), 2057–66.

11. Schulte F.A., Lambers F.M., Kuhn G., Müller R. In vivo micro-computed tomography allows direct three-dimensional quantification of both bone formation and bone resorption parameters using time-lapsed imaging. *Bone*. 2011;48(3), 433–42.

12. Schulte F.A., Ruffoni D., Lambers F.M., Christen D., Webster D.J., Kuhn G., et al. Local Mechanical Stimuli Regulate Bone Formation and Resorption in Mice at the Tissue Level. *PLoS One*. 2013;8(4), E62172.

13. Ellouz R., Chapurlat R., Van Rietbergen B., Christen P., Pialat J.-B., Boutroy S. Challenges in longitudinal measurements with HR-pQCT: Evaluation of a 3D registration method to improve bone microarchitecture and strength measurement reproducibility. *Bone*. 2014;63, 147–57.

14. Christen P., Ito K., Ellouz R., Boutroy S., Sornay-Rendu E., Chapurlat R.D., et al. Bone remodelling in humans is load-driven but not lazy. *Nat Commun*. Nature Publishing Group; 2014;5, 1–5.

15. Christen P., Boutroy S., Ellouz R., Chapurlat R., Van Rietbergen B. Least-detectable and age-related local in vivo bone remodelling assessed by time-lapse HR-pQCT. *PLoS One*. 2018;13(1), 1–11.

16. Hartley C., Folland J.P., Kerslake R., Brooke-wavell K. High-Impact Exercise Increased Femoral Neck Bone Density With No Adverse Effects on Imaging Markers of Knee Osteoarthritis in Postmenopausal Women. 2020;35(1), 53–63.

17. Clarke B. Normal bone anatomy and physiology. *Clin J Am Soc Nephrol*. 2008;3 Suppl 3, 131–9.

18. Eleftheriou K.I., Rawal J.S., Kehoe A., James L.E., Payne J.R., Skipworth J.R., et al. The Lichfield bone study: the skeletal response to exercise in healthy young men. *J Appl Physiol*. 2012;112(4), 615–26.

19. Sornay-Rendu E., Boutroy S., Munoz F., Delmas P.D. Alterations of cortical and trabecular architecture are associated with fractures in postmenopausal women, partially independent of decreased BMD measured by DXA: The OFELY study. *J Bone Miner Res*. 2007;22(3), 425–33.

20. Paggiosi M.A., Eastell R., Walsh J.S. Precision of high-resolution peripheral quantitative computed tomography measurement variables: Influence of gender, examination site, and age. *Calcif Tissue Int*. 2014;94(2), 191–201.

21. Metcalf L.M., Dall'Ara E., Paggiosi M.A., Rochester J.R., Vilayphiou N., Kemp G.J., et al. Validation of calcaneus trabecular microstructure measurements by HR-pQCT. *Bone*.; 2018;106, 69–77.

22. Du J., Brooke-Wavell K., Paggiosi M.A., Hartley C., Walsh J.S., Silberschmidt V. V., et al. Characterising variability and regional correlations of microstructure and mechanical competence of human tibial trabecular bone: An in-vivo HR-pQCT study. *Bone*. Elsevier; 2019;121(January), 139–48.

23. Singh A.K., Lobo Gajiwala A., Rai R.K., Khan M.P., Singh C., Barbhuyan T., et al. Cross-correlative 3D micro-structural investigation of human bone processed into bone allografts. *Mater Sci Eng C*. 2016;62, 574–84.

24. Doube M., Kłosowski M.M., Arganda-Carreras I., Cordelières F.P., Dougherty R.P., Jackson J.S., et al. BoneJ: Free and extensible bone image analysis in ImageJ. *Bone*. 2010 Dec;47(6), 1076–9.

25. Hildebrand T., Rüegsegger P. A new method for the model-independent assessment of thickness in three-dimensional images. *J Microsc*. 1997;185(1), 67–75.

26. Whittier D.E., Boyd S.K., Burghardt A.J., Paccou J., Chapurlat R., Engelke K. Guidelines for the assessment of bone density and microarchitecture in vivo using high-resolution peripheral quantitative computed tomography. 2020;

27. Lorensen W.E., Cline H.E. MARCHING CUBES: A HIGH RESOLUTION 3D SURFACE CONSTRUCTION ALGORITHM. *ACM siggraph Comput Graph*. 1987;21(4), 163–9.

28. Doube M. The ellipsoid factor for quantification of rods, plates, and intermediate forms in 3D geometries. *Front Endocrinol (Lausanne)*. 2015;6, 15.

29. Chai X., van Herk M., Hulshof M.C.C.M., Bel A. A voxel-based finite element model for the prediction of bladder deformation. *Med Phys*. John Wiley & Sons, Ltd; 2011 Dec 9;39(1), 55–65.

30. Klintström E., Klintström B., Moreno R., Brismar T.B., Pahr D.H., Smedby Ö. Predicting Trabecular Bone Stiffness from Clinical Cone-Beam CT and HR-pQCT Data: An In Vitro Study Using Finite Element Analysis. *PLoS One*. 2016;11(8), E0161101.

31. Burr D.B., Milgrom C., Fyhrie D., Forwood M., Nyska M., Finestone A., et al. In vivo measurement of human tibial strains during vigorous activity. *Bone*. 1996;18(5), 405–10.

32. Lim C.T., Ng D.Q.K., Tan K.J., Ramruttun A.K., Wang W., Chong D.Y.R. A biomechanical study of proximal tibia bone grafting through the lateral approach. *Injury*. Elsevier Ltd; 2016;47(11), 2407–14.

33. Christen P., Müller R. In vivo Visualisation and Quantification of Bone Resorption and Bone Formation from Time-Lapse Imaging. *Curr Osteoporos Rep*. Current Osteoporosis Reports; 2017;15(4), 311–7.

34. Lambers F.M., Kuhn G., Weigt C., Koch K.M., Schulte F.A., Müller R. Bone adaptation to cyclic loading in murine caudal vertebrae is maintained with age and directly correlated to the local micromechanical environment. *J Biomech*. Elsevier; 2015;48(6), 1179–87.

35. Burghardt A.J., Kazakia G.J., Sode M., De Papp A.E., Link T.M., Majumdar S. A longitudinal HR-pQCT study of alendronate treatment in postmenopausal women with low bone density: Relations among density, cortical and trabecular microarchitecture, biomechanics, and bone turnover. *J Bone Miner Res*. 2010;25(12), 2282–95.

36. Eriksen E.F., Melsen F., Sod E., Barton I., Chines A. Effects of long-term risedronate on bone quality and bone turnover in women with postmenopausal osteoporosis. *Bone*. 2002;31(5), 620–5.

37. Recker R.R., Weinstein R.S., Chesnut C.H., Schimmer R.C., Mahoney P., Hughes C., et al. Histomorphometric evaluation of daily and intermittent oral ibandronate in women with postmenopausal osteoporosis: Results from the BONE study. *Osteoporos Int*. 2004;15(3), 231–7.

38. Burt L.A., Liang Z., Sajobi T.T., Hanley D.A., Boyd S.K. Sex- and Site-Specific Normative Data Curves for HR-pQCT. *J Bone Miner Res*. 2016;31(11), 2041–7.

39. Shanbhogue V. V, Brixen K., Hansen S. Age- and Sex-Related Changes in Bone Microarchitecture and Estimated Strength: A Three-Year Prospective Study Using HRpQCT. *J Bone Miner Res*. 2016 Aug;31(8), 1541–9.

40. Whittier D.E., Burt L.A., Hanley D.A., Boyd S.K. Sex- and Site-Specific Reference Data for Bone Microarchitecture in Adults Measured Using Second-Generation HR-pQCT. *J Bone Miner Res*. 2020;

41. Gabet Y., Bab I. Microarchitectural changes in the aging skeleton. *Curr Osteoporos Rep*. 2011;9(4), 177–83.

42. Sundh D., Nilsson M., Zoulakis M., Pasco C., Yilmaz M., Kazakia G.J., et al. High Impact Mechanical Loading Increases Bone Material Strength in Postmenopausal Women - a 3-Month Intervention Study. *J Bone Miner Res*. 2018;33(7), 1242–51.

43. Lai Y.M., Qin L., Yeung H.Y., Lee K.K.H., Chan K.M. Regional differences in trabecular BMD and micro-architecture of weight-bearing bone under habitual gait loading - A pQCT and microCT study in human cadavers. *Bone*. 2005;37(2), 274–82.

44. Chen H., Zhou X., Fujita H., Onozuka M., Kubo K. Age-Related Changes in Trabecular and Cortical Bone Microstructure. *Int J ofEndocrinology*. 2013;2013(213234).

45. Ding M., Hvid I. Quantification of age-related changes in the structure model type and trabecular thickness of human tibial cancellous bone. *Bone*. 2000;26(3), 291–5.

46. Parkinson I.H., Fazzalari N.L. Characterisation of Trabecular Bone Structure. In: Stud Mechanobiol Tissue Eng Biomater. 2013. p. 31–51.

47. Liu X.S., Sajda P., Saha P.K., Wehrli F.W., Bevill G., Keaveny T.M., et al. Complete Volumetric Decomposition of Individual Trabecular Plates and Rods and Its Morphological Correlations With Anisotropic Elastic Moduli in Human Trabecular Bone. *J Bone Miner Res*. 2007;23(2), 223–35.

48. Bailey C.A., Brooke-Wavell K. Optimum frequency of exercise for bone health: Randomised controlled trial of a high-impact unilateral intervention. *Bone*. Elsevier Inc.; 2010;46(4), 1043–9.

49. Cheung A.M., Adachi J.D., Hanley D.A., Kendler D.L., Davison K.S., Josse R., et al. High-resolution peripheral quantitative computed tomography for the assessment of bone strength and structure: A review by the canadian bone strength working group. *Curr Osteoporos Rep*. 2013;11(2), 136–46.

50. Chantal M. J. de Bakker, Allison R. Altman, Connie Li, Mary Beth Tribble, Carina Lott, Wei- Ju Tseng and X.S.L. Minimizing Interpolation Bias and Precision Error in In Vivo μCT- based Measurements of Bone Structure and Dynamics. *Ann Biomed Eng*. 2016;44(8), 2518–28.

Appendix I: Rates of bone formation (tBFR) and resorption (tBRR) per month between EL and CL for each RVE to demonstrate local variation.

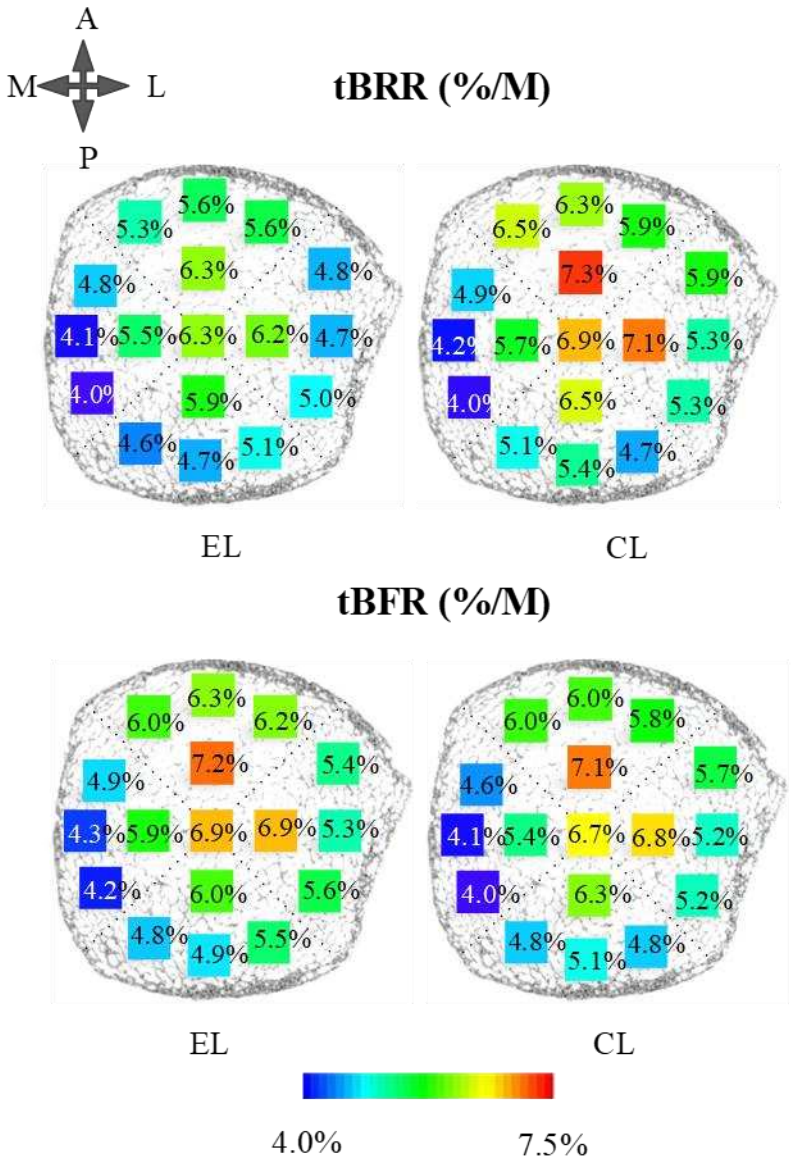

Appendix II: Mean difference in BV/TV, Tb.Th, Tb.SP, Tb.N, Tb.BS, $_{P}$Tb.N/$_{T}$Tb.N and stiffness of each RVE between pre- and post-intervention for EL and CL.